공학석사 학위논문

출력 토크 조절이 가능한 Scotch yoke 메커니즘

An adjustable Scotch yoke mechanism for output torque regulation

2013년 2월

서울대학교 대학원

기계항공공학부

권 석 령

Abstract

An adjustable Scotch yoke mechanism for output torque regulation

Seok-Ryung Kwon

School of Mechanical and Aerospace Engineering

The Graduate School

Seoul National University

The robotic fish using servomotor was generally difficult to operate high frequency because the servo motor decreases the velocity to switch the direction of the tail fin. To solve this problem, various researchers have tried to use the Scotch yoke mechanism with DC motor for robotic fish. The Scotch yoke mechanism converts the rotating motion of motor into the reciprocating motion. However, in this mechanism, the torque of the motor with scotch yoke mechanism is changed in terms of the phase of the tail fin while the DC motor maintains the torque constantly. Thus, the objective of this paper is to regulate the motor output torque by using the adjustable Scotch yoke mechanism. This mechanism uses springs to store the motor torque and cam mechanism to release this torque at desired moment. We analyzed a kinematic model of the Scotch yoke mechanism to propose a method of designing the part of the adjustable Scotch yoke mechanism. In addition, we experiment to measure the thrust of tail fin while the equal input voltage of controller is supplied respectively and compare the conventional mechanism and

adjustable Scotch yoke mechanism by considering the compliance of the fin. As a result, we conclude that the adjustable scotch yoke mechanism enables the propulsion system to improve the average thrust than conventional scotch yoke mechanism during the equivalent power consumption. Therefore, based on these result, the high speed robotic fish can be made by applying the adjustable Scotch yoke mechanism which regulated the output torque.

Keywords: Scotch yoke mechanism, Robotic fish, Propulsion system, Torque regulation

Student Number: 2011-20683

Contents

List of Tables

List of Figures

Chapter 1. Introduction

In recent years, there has been growing interests in bio-inspired robotic fish for exploring the sea and collecting resources. Biomimetic propulsion system is better in terms of power consumption and maneuverability than conventional propeller propulsion system [1]. Because of these advantages, biomimetic robotic fish have been studied extensively during the past two decades.

In general, the field of robotic fish is relatively proceeding on the mimicking the biological fish such as swimming motion and specific shape. The Robotuna using six servo motors is the first robotic fish developed by MIT [2]. Hu designed the multi joint robotic fish G9 which is exhibited at the London Aquarium [3]. This robotic fish is swimming like a real fish by performing natural undulation motion and the outstanding design. Low *et al.* designed a Roman inspired by manta ray which is swimming like a flapping, undulation and gliding, driven by eight servo motors in series [4]. A multilink dolphin-like robot which moves dorsoventral motion achieves better performance for pitch maneuvers [5]. Recently, the batoid robot, a prototype of a field deployable biomimetic stingray was developed by Alvarado *et al.* [6]. Moreover, various researchers of the robotic fish not only mimicked the biological character of fish, but also proposed more attractive, more efficient studies to have with better performance. Park *et al*. have experimented that the compliance of a fin affects the thrust of robotic fish [7]. They proved that the *half-pi phase delay* condition for maximizing the thrust generated by a

compliant fin propulsion system. Alvarado *et al*. designed the robotic fish to mimic the kinematics of real fish and their swimming techniques, by using undulation derived from compliance of their bodies [8-9]. This study showed that the simple design using one servo motor can be achieved showing the undulation motion sufficiently similar to the robotic fish which actuated by the several servo motors. Lauder *et al*. used the various robotic caudal fins to test the effects of fin ray stiffness, frequency, and motion program on the generation of thrust and lift forces [10-11]. The cupping motion generated the thrust greater than other motion such as flat, undulation, and W shape and rolling. Low *et al*. conducted the experiment to investigate the swimming performance of robotic fish by using a various design parameters [12]. They showed that the frequency and amplitude were important parameters on the thrust of the robotic fish. It was noted that the thrust of robotic fish is increased as the frequency rose within the specific frequency. However, robotic fish using servomotor was difficult to generate high frequency due to lack of proper amount of torque and the restraint of the response time. To solve this problem, some researchers have tried to use the Scotch yoke mechanism with DC motor for robotic fish. The Scotch yoke mechanism converts the revolution of motor into the reciprocating motion. In this mechanism, the DC motor maintains the constant velocity while the servo motor decreases the velocity to switch the direction of the tail fin. Thus, the Scotch yoke mechanism makes the tail fin operate the high frequency. Park *et al*. has conducted various experiments to figure out correlation between thrust and frequency of tail fin [13]. They found that the frequency for the maximum

thrust increased up to the 10 Hz when the Scotch yoke mechanism was used. Junzhi Yu *et al*. designed the RoboDolphin –III which used the Scotch yoke mechanism and compared the performance of the thrust between robotic fish which used servo motors and RoboDolphin –III [14]. This study showed that the robotic fish using the Scotch yoke mechanism is operating properly at higher frequency than robotic fish using servo motors. However, this method also drives limited maximum frequency when the large torque is applied to the motor. So far, there is an insufficient study of overcoming the this phenomenon in propulsion system with Scotch yoke mechanism, except for the research which simply changes amplitude and the trajectory of the Scotch yoke mechanism [15-19].

In order to overcome this limitation of the frequency, the motor torque is the important factor. Especially, the torque applied to the motor is not constant in the fin propulsion system caused by the features of the Scotch yoke mechanism. We focus on this characteristic to use the Scotch yoke mechanism more efficiently.

The objective of this paper is to regulate the motor output torque by using the adjustable Scotch yoke mechanism. This mechanism uses springs to store the motor torque and cam mechanism to release this torque at desired moment. In this paper, we use a kinematic model that explained the required torque and the actual torque of motor using the Scotch yoke mechanism to obtain the design parameters. Moreover, we develop the adjustable Scotch yoke mechanism based on the design parameters and compare the previous mechanism and new mechanism in constrained condition. We conduct the

experiments to measure the thrust while the equal input voltage of controller is provided respectively. In addition, the thrust and the angle position of the tail fin is analyzed to confirm the performance of the adjustable Scotch yoke mechanism. The experimental result shows that for a limited torque condition, the adjustable Scotch yoke mechanism increases the thrust considerably. Therefore, the adjustable Scotch yoke mechanism can be used for a robotic fish with high speed and high efficiency.

Chapter 2. The Propulsion System with Scotch Yoke Mechanism

2.1 Characteristics of the Scotch Yoke Mechanism

In this section, we explain the features of the Scotch yoke mechanism. The Scotch yoke mechanism changes a rotary motion to a reciprocating motion. Thus, this mechanism can use the DC motor which has the high speed velocity. This advantage induces the movement of tail fin to move faster. Fig. 2.1 shows the movement of the Scotch yoke mechanism. The rotating motion of crank wheel is translated to an up-and-down motion.

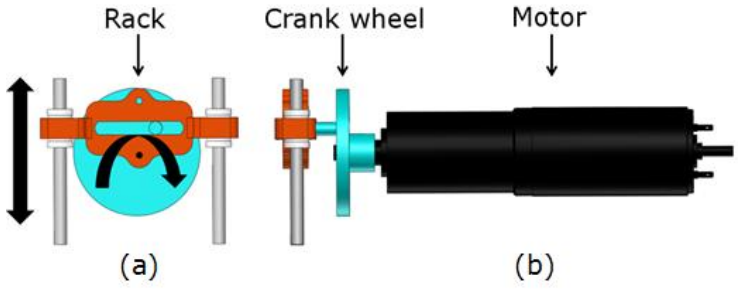

Fig. 2.1. Overall design of the Scotch yoke mechanism. (a)front view (b) side view

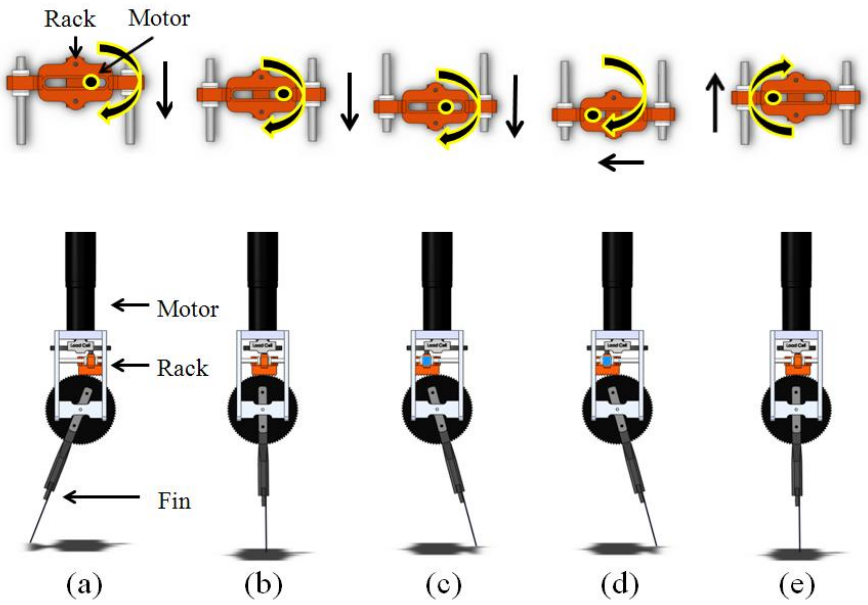

Fig. 2.2. Schematic drawing of the Scotch yoke mechanism: the top is the motion of the rack, and the bottom is the movement of the tail fin when (a) the rack is in the top, (b) the rack moves to the bottom, (c) rack is in the bottom, (d) the rack changes of the direction, (e) the rack moves to the top.

Fig. 2.2 describes the change of the location of the tail fin depending on the movement of the crank wheel. The rack moves up and down while, the crank wheel rotates along the ellipsoidal hole of the rack. The gear of the rack spins the round gear which is connected to the tail fin. As a result, the tail fin moves from one end to the other end, while the rack moves up and down. During this process, the drag force is applied to the tail fin and torque is also applied to the motor. We defined that this torque is the required torque. There are noticeable characteristic about the required torque. The required torque does not maintain consistently while the motor rotates. Especially, the crank

wheel does not move the rack while the tail fin changes the direction of the movement. In this process, the required torque is smaller than other conditions. In contrast, the required torque is the largest when the tail fin passes the center. If the torque of the motor is not enough to meet the required torque, the motor does not work properly. Moreover, the velocity of the motor is influenced by the torque of the motor. Thus, the movement of the tail fin is affected by the torque of the motor. Because of this phenomenon, the motor torque is an important factor in the Scotch yoke mechanism. Therefore, we are interested in the method to control the motor torque which influences the movement of the tail fin, and the features of the Scotch yoke mechanism are analyzed.

2.2 Kinematic Model of Scotch Yoke Mechanism

We designed the kinematic model of the Scotch yoke mechanism as illustrated in Fig. 2.3

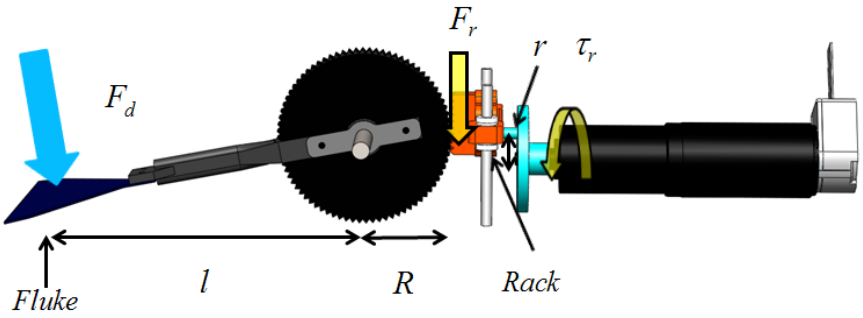

Fig. 2.3 Kinematic analysis of the Scotch yoke mechanism

Given the simulation parameter, the torque of the motor can be calculated analytically by solving the equations as follows:

$$y_{Rack} = r\sin\omega t\,, \tag{2.1}$$

$$v_{Rack} = r\omega\cos\omega t\,, \tag{2.2}$$

$$v_{Fluke} = \frac{l}{R}v_{Rack} = \frac{l}{R}l\omega\cos\omega t\,, \tag{2.3}$$

$$F_d = \frac{1}{2}\rho {v_{fluke}}^2 C_d A = \frac{1}{2}\rho C_d A\left(\frac{r}{R}l\omega\cos\omega t\right)^2, \tag{2.4}$$

$$F_r = F_d\frac{l}{R} = 2\pi^2\rho C_d A\frac{r^2}{R^3}l^3 f^2\cos^2(2\pi ft)\,, \tag{2.5}$$

$$\tau_r = F_r \cdot r\cos\omega t = 2\pi^2 \rho C_d A\left(\frac{r}{R} l\cos(2\pi ft)\right)^3 \cdot f^2 . \qquad (2.6)$$

where the F_d indicates the drag force toward the tail fin, and F_r indicates the force that acts on the motor. From the equations, the required torque (τ_r) of the motor can be expressed in terms of the frequency of the tail fin. From the equation (6), we confirm that the required torque does not stabilize consistently. On the contrary, the torque (τ_m) of the motor is constant because the maximum capable torque of the motor is fixed. The numerical value for the model is shown in Table 2.1. The equations are simulated by MATLAB function file that describes the required torque when given the numerical value like Table 2.1.

Table 2.1 The simulation parameters

Density of water(ρ)	1000 kg/m^3
Drag coefficient of a flat plate(C_d)	1.28
Area of the fin(A)	4000×10^{-6} m^2
Radius of gear(R)	40×10^{-3} m
Radius of crank wheel(r)	15×10^{-3} m
Length of the link(l)	17×10^{-2} m

Fig. 2.4 (a) shows that the required torque from the equation (6) and torque created by the motor. The required torque is similar to the sinusoidal graph which is expressed using the MATLAB function file. The solid line describes the torque of the motor and the dotted line shows the required torque. In this graph, the more the frequency of tail fin increased, the more the amplitude of the required torque rose. Thus, the required torque is larger than the torque of the motor when the frequency of the tail fin is too high. In this variation, the velocity of the motor is decreased since the torque is insufficient. As a result, the frequency of the tail fin does not increase above

the constant value and the thrust is constrained. To solve this problem, we studied the method of increasing the toque of the motor when the required torque is higher than the maximum capable torque of the motor. First of all, we take note of the period which is in the low required torque condition. Thus, to increase the final motor torque, we use the springs which can stores a motor torque in the low required torque condition. The saved torque is released in the high required torque condition. In addition, we consider the cam mechanism to regulate the phase of the torque from the springs, because of the phase difference between low required torque condition and inverse case.

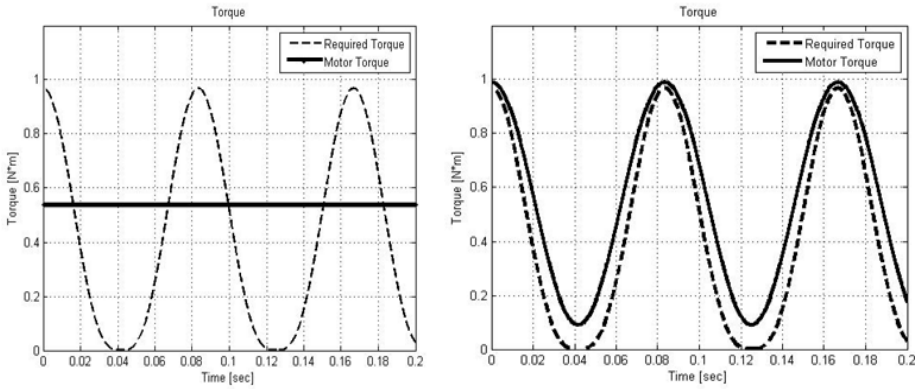

Figure. 2.4. Comparison between the motor torque and the required torque in specific frequency (6 Hz) (a) Common Scotch yoke mechanism (b) Adjustable Scotch yoke mechanism.

Therefore, we develop the adjustable Scotch yoke mechanism which can regulate the output torque. This mechanism saves the torque from the motor into the springs when the required torque is relatively low, and releases the torque while the motor needs the high torque. In details, the adjustable Scotch yoke mechanism stores the torque into the springs by using the curved shape crank wheel. After that, the stored torque is added to the necessary condition when the high torque is required. As a result, we obtain the sinusoidal graph of torque of the motor similar with the graph of the required torque as shown in Fig. 2.4 (b).

Chapter3. Adjustable Scotch Yoke Mechanism

3.1 Design of Adjustable Scotch Yoke Mechanism

In order to develop the adjustable output torque regulation mechanism, we invented a new kind of device as illustrated in Fig. 3.2. In addition, to regulate the phase of the motor torque, we change the previous crank wheel to the new one. Fig.3.1 shows that the design of the crank wheel is translated the circle shape to the number 8 shape.

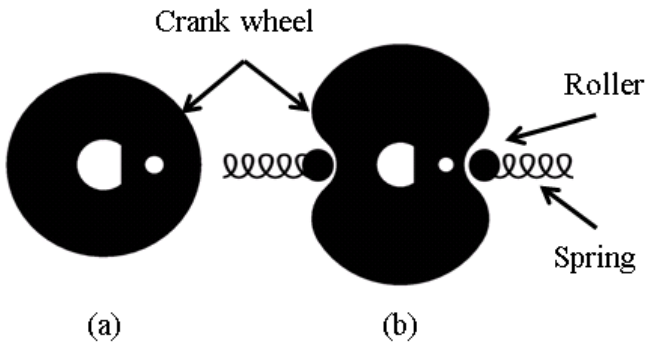

Figure. 3.1. The design of the crank wheel (a) Previous crank wheel (b) New crank wheel.

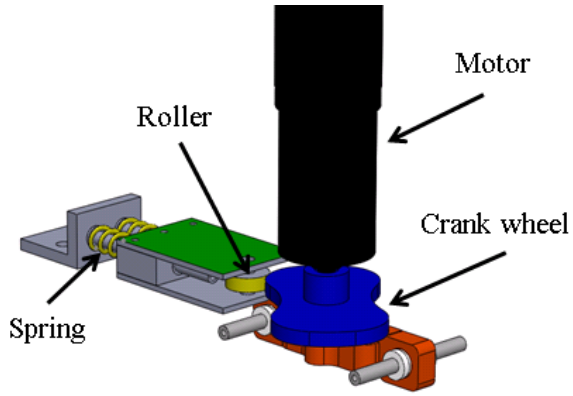

Figure. 3.2. The First design of the adjustable Scotch yoke mechanism with springs.

The adjustable Scotch yoke mechanism is composed of the crank wheel, the rollers, and the springs. The crank wheel has the curved shape to push the rollers. The rollers which are faced to the crank wheel move side to side, and the springs are compressed along to the rod. In this progress, the torque of the motor is stored in the springs. When the motor starts to rotate, the contact point changes according to the surface of the crank wheel because the crank wheel is designed as the curved shape in order to make the sinusoidal torque graph. However, the first design is difficult to apply to the robotic fish because this design requires the large cross section area. To solve this problem, we develop the innovation design inspired from the variable stiffness mechanism designed by Wolf and Hirzinger [20]. In order to design more compactly, we changed the conventional crank wheel to the curved shape crank wheel as shown in Fig. 3.4. In the curved shape crank wheel, the rollers move along to the surface in parallel with the axis of the motor.

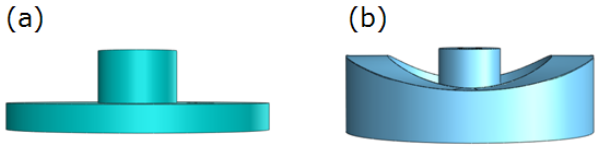

Figure. 3.3 Crank wheel side view (a) Conventional crank wheel (b) Curved shape crank wheel.

The difference between the first design and the final design is the shape of the crank wheel. In addition, this shape is determined by the maximum capable torque of the motor. The design of the crank wheel will be explained precisely in the next chapter.

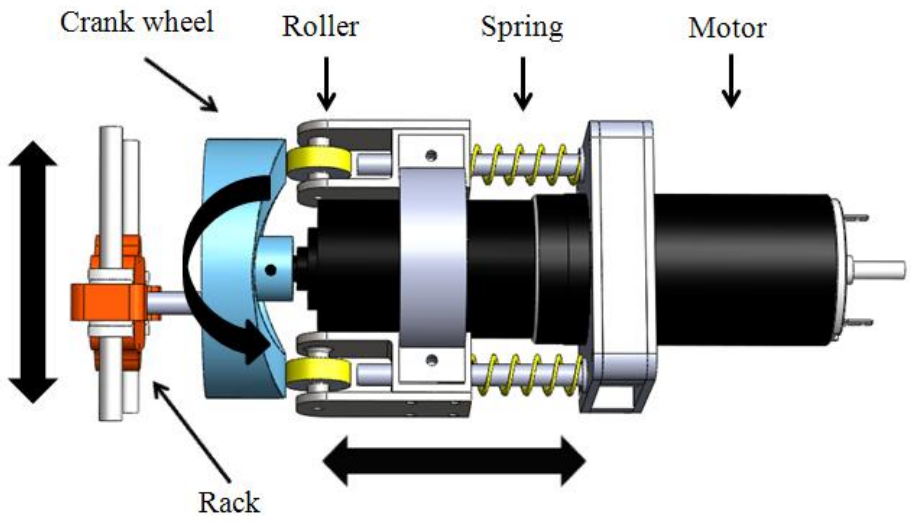

Figure. 3.4 The components of the adjustable Scotch yoke mechanism.

The output torque of the motor is changed by this mechanism, while the rollers move along the surface of the crank wheel from side to side. After the released torque from the springs is added to the maximum capable torque, the final torque of the motor can be higher than the required torque. As a result, we obtain the similar torque profile with the required torque and control the final output torque using this mechanism.

3.2 Modeling of the Crank Wheel

As shown in Fig. 3.3, we change the original crank wheel to the curved shape crank wheel for making the graph as the required torque. As seen Fig. 3.5, the surface of the crank wheel is designed as follows:

$$F_T R = B\sin 2\theta, \tag{3.1}$$

$$F_k = k(h - ho), \tag{3.2}$$

$$\tan\alpha = \frac{F_T}{F_k} = \frac{dh}{Rd\theta}, \tag{3.3}$$

$$F_k dh = F_T R d\theta, \tag{3.4}$$

$$k(h - ho)dh = B\sin 2\theta d\theta, \tag{3.5}$$

$$h^2 - 2hho + C + \frac{B}{k}\cos 2\theta = 0, \tag{3.6}$$

$$h = ho + \sqrt{ho^2 - \frac{B}{k}\cos 2\theta}\ . \tag{3.7}$$

where F_k indicates the elasticity force toward the y axis, and F_T indicates the rotational force toward the x axis. In addition, F_n indicates the force towards the direction perpendicular to the x and y axes. The height (h) of the surface of crank wheel is derived from the equation (13). We excluded the frictional force between the rollers and the crank wheel, since the friction coefficient is relatively small. Moreover, the constant C is assumed to be zero for convenience of calculation.

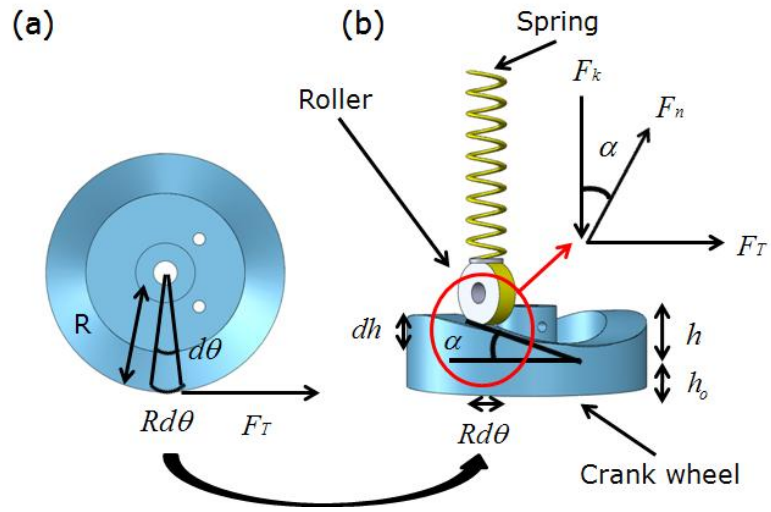

Figure. 3.5 Free body diagram of crank wheel (a) Front view (b) Side view.

To design the path of the crank wheel precisely, we consider the influence of the rollers as seen in Fig. 3.6 (a). Due to the radius of the rollers, the equation of the height can be described as follows:

$$h' = h - r\cos\alpha\,, \tag{3.8}$$

From equation (9)

$$\tan\alpha = \frac{dh}{Rd\theta} = \frac{B\sin 2\theta}{k\sqrt{ho^2} - \frac{B}{K}\cos 2\theta}\,, \tag{3.9}$$

$$\cos\alpha = \frac{1}{\sqrt{1+\tan^2\alpha}}\,. \tag{3.10}$$

Using these equations, we design the shifted path of the surface of the crank wheel.

With the change of the height, the phase of the angle is considered as follows:

$$\theta' = \theta - \frac{r}{R}\sin\alpha\,, \tag{3.11}$$

$$\sin\alpha = \frac{1}{\sqrt{1+\cot^2\alpha}}\,. \tag{3.12}$$

Where, indicates h the path of rollers, h' indicates the path of the shifted height, and α indicates the angle between the surface of the crank wheel and the y axis. In addition, θ indicates the angle position of the crank wheel, and θ' indicates the shifted angle cause by the radius of the rollers. However, the change of the angle does not influence the design of the crank wheel because the radius of roller is smaller than that of the crank wheel.

The equations are simulated by MATLAB function file that describes the displacement of the crank wheel when given the maximum torque (B), spring constant (k), and compression condition (h_0). Fig. 3.6 (b) shows the path of crank wheel in consideration of the influence of the roller when the design data are input using MATLAB function file. The red solid line is the path of the center of the rollers, the blue dotted line is the path of the shifted height, and the green solid line is the path of the shifted angle.

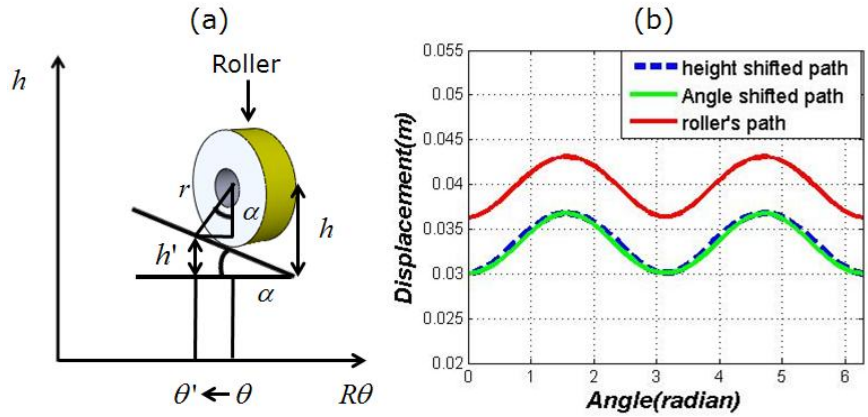

Figure. 3.6 (a) Kinematic analysis of crank wheel path with considered roller
(b) Design parameter of crank wheel (B: 0.4Nm, k=3N/m r=6.5mm).

3.3 Design of the Scotch Yoke Mechanism

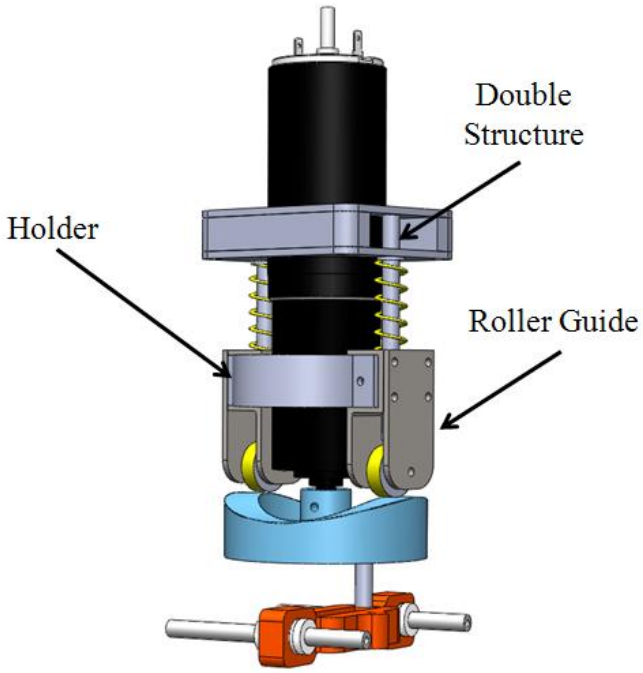

Figure. 3.7 The design consideration of the moment and torsion.

With the design of crank wheel, we deign the adjustable Scotch yoke mechanism by considering the several elements. First of all, to prevent the moment of the rod, the double structures installed as illustrated in Fig 3.7. In addition, the holders which attach the roller guide setup in order to reduce the twisting moment of the Roller Guide.

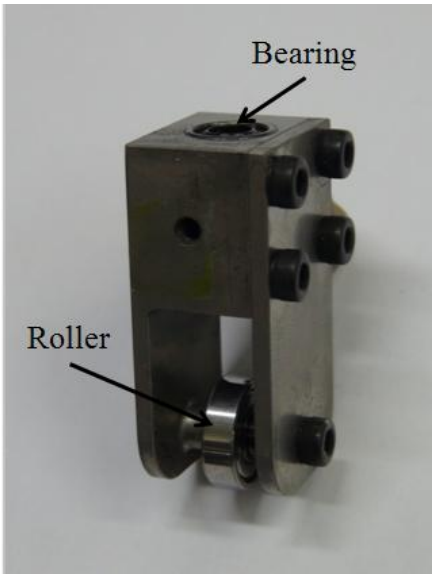

Figure. 3.8 The Roller Guide with the Roller and Bearing.

As shown in Fig. 3.8, the Bearing is inserted to the Roller Guide. This bearing enables the Roller Guide to move along to the rod smoothly. The Roller is an interference fit with the Roller Guide. Thus the Roller can be maintaining the center of the Roller Guide. With consideration of various design elements, we installed the experimental setup in a small water tank.

Chapter 4. Method

4.1 Experimental Procedure

In order to test the feasibility of the concept, the tests were performed in the apparatus explained in Table 4.1 and described in Fig. 4.1.

Table 4.1 Specification of the apparatus

Water tank	700mm×320mm×520mm
experimental setup	190mm×160mm×450mm
Weight	1500g
Compression springs	1.5N/mm
Motor	Maxon DC Brushes motor
Power source	200 W Power supply

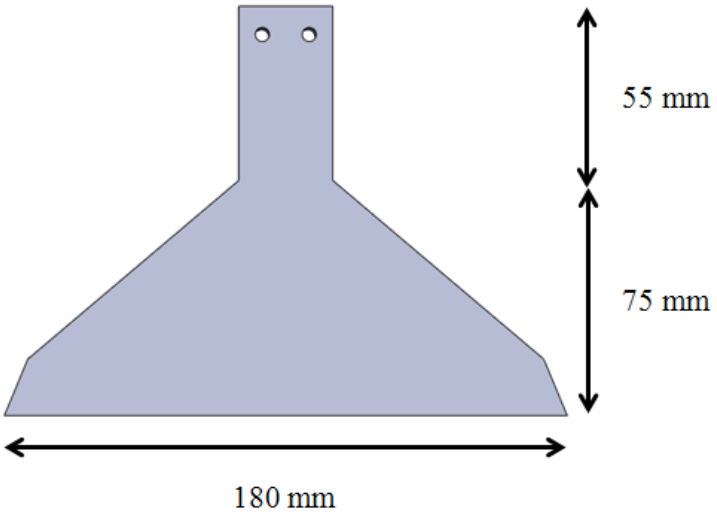

Figure. 4.1 The design of the tail fin.

The shape and size of the tail fin is illustrated in Fig. 4.1. This fin is manufactured by attaching the 13 carbon fiber sheets which is good stiffness materials. The size of the tail fin is determined to experiment in the small water tank. Moreover, due to the restriction of the size of the water tank, the tail fin flaps with relatively low frequency. In order to experiment under this condition, the motor torque is constrained by setting the maximum current of the motor. To decide the maximum torque of the motor, the current is restricted under the 930mA and the maximum torque is calculated by Table 4.2.

Table 4.2 Torque parameter

Maximum current	930mA
Torque constant	29.2mNm/A
Maximum torque	$29.2 \times 0.93 \times 5.8 = 0.157$Nm

Based on the maximum torque from the Table 4.2 the crank wheel can be designed. Furthermore, we manufactured the adjustable Scotch yoke mechanism by assembling the crank wheel, the springs, and the rollers. We measured the thrust, displacement, current of the motor, and the period of the tail fins according to the change of the input voltage. Moreover, we compared the Conventional mechanism and the adjustable Scotch yoke mechanism.

4.2 Apparatus

The experimental setup with two load cells (Ktoyo 333FB) which collect data of thrust as illustrated in Fig.4.2. (a).

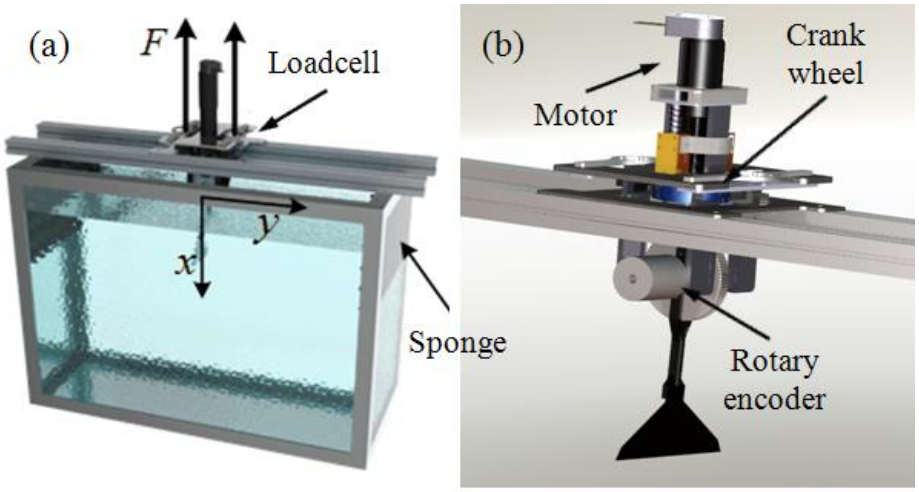

Figure. 4.2 Schematics design of the experimental setup. (a) Experiment water tank with load cell (b) Adjustable Scotch yoke mechanism.

In addition, the sponges are attached at both side of the water tank to prevent the influence of the flow.

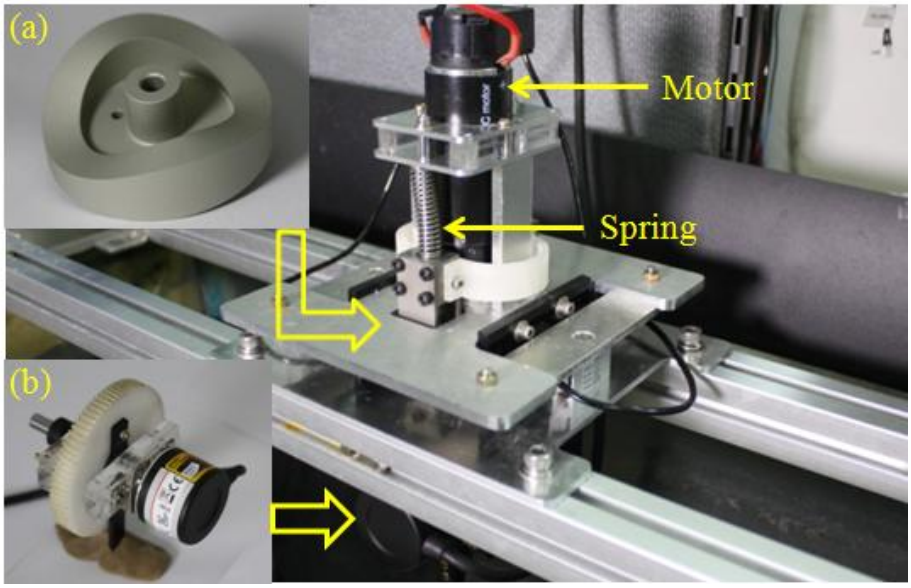

Figure. 4.3 Experimental setup (a) Crank wheel (b) Rotary encoder (LS mecapion FH40).

The tail fin position is measured by rotary encoder as illustrated in Fig 4.2. (b). The thrust of load cell data is processed by National Instrument CompactRIO DAQ 9237 which is measured at 2000 samples/s. The total force is summing the two sets of force data since the two load cell are parallel in the y-axis. Fig. 4.3 shows the crank wheel (a) which made by the design parameter from the equations, and rotary encoder (b) which measures the angle of the tail fin. The Casio EX FH-100 High Speed Camera a setup in front of the water tank to record the movement of the tail fin at 480frames/s.

Chapter 5. Results and Discussion

5.1 Experimental Result

The results of the experiment differ according to the use of the springs. The case when springs are used is denoted by S and the case when springs are not used is denoted by NS. The results are compared between S and NS, while the velocity of the motor is increased by changing the input voltage of the controller from 3V to 4V. Table 5.1 shows the thrust for each condition during the one cycle of the movement of the tail fin.

Table 5.1 Experiment result

Condition	Thrust(mN)
Non Spring 3	509
Non Spring 3.5	502
Non Spring 4	502
Spring 3	582
Spring 3.5	607
Spring 4	579

From Table 5.1, in the result of the thrust, the case with springs increased the thrust from 13.7 to 21.0 percent although the consumed current is 930mA in each condition. As a result, the S case has more energy efficient mechanism than the NS case.

5.2 Analysis of the Experimental Results

The graphs of the experimental result comparing S and NS are illustrated in Fig. 5.1. The solid black line describes the S case and the dotted red line shows the NS case. Because the S case of the frequency is faster than the NS case, the period of the solid black line is shorter than that of the red line. Fig. 5.1 (a) shows the motion of the tail fin during one cycle. In the adjustable Scotch yoke mechanism, the motor torque is stored to the springs when the tail fin switches the direction (from 0.2s to 0.3s). This area is less important than center area to generate the thrust. After that, the stored motor torque from the springs is released when the required torque is increased. Note that when the tail fin passes the center area (from 0.4s to 0.6s), the velocity of the NS case decreases sharply since the torque of the motor is insufficient to move the tail fin. Because the difference of the velocity influences the thrust of the tail fin, the thrust of the NS case is declined drastically in the equivalent period as shown Fig. 5.1(b). In this area, the thrust of the NS case drops almost zero. Conversely, the S case maintains the velocity of the tail fin relatively because the stored motor torque helps the motor to move the tail fin. Thus, the S case which added the torque from the springs is enough to move the tail fin in the equal area and the tail fin passes the center position more quickly in the S case. In this area, the thrust of the S case maintains high state versus the NS case. As a result, the average thrust of the S case is better than the NS case since the thrust of the S case maintains high state versus the NS case.

However, we found the unexpected phenomenon in the Fig 5.1. First of all, the maximum thrust point of the NS case is higher than the S case at the 0.4 seconds. This phenomenon is occurred that the velocity of the NS case is faster than the S case while the tail fin switches the direction. The S case is difficult to increase the velocity such as the NS case since the motor is influenced by compressing the springs in this area. Therefore, the thrust of the NS case increases more than the S case until the velocity of the NS case start to drop. Secondly, in the angle position of the Fig 5.1 (b), the tail fin of the NS case returns the previous position at the 0.4 second. From the analysis of the video from high speed camera, the velocity is almost zero; this phenomenon is occurred when bending of the fin is unfolded. The reaction force from the tail fin is applied to the peduncle which is connected between motor and tail fin. In this phenomenon, the velocity of the NS case is changed into the negative value.

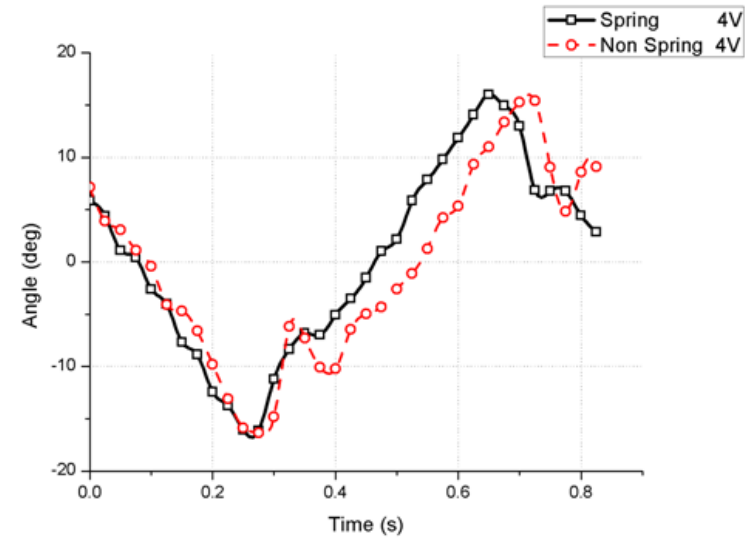

(a)

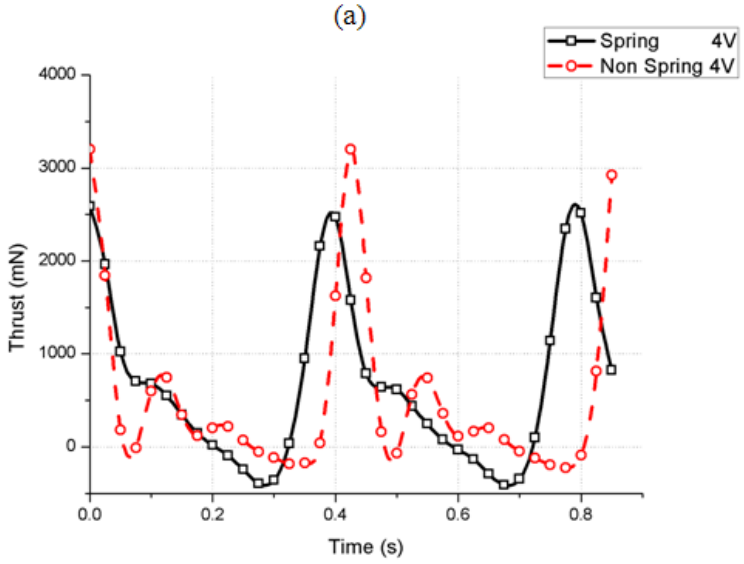

(b)

Figure. 5.1 Graphical synopsis of experimental result (Comparison the thrust and the angle position between S and NS at the 4V (a) The angle displacement of result (b) The thrust result.

In addition, we experiment the more rigid tail fin to investigate if the compliance of the tail fin influence to the experimental result. To manufacture the rigid tail fin, the thickness is increased by attaching more eight carbon fiber sheets. Thus, the carbon fiber sheets of rigid fin are 20 and the stiffness rigid value is 907 N/m. This stiffness is four times as stiff as the compliance fin since stiffness of compliance fin is 196 N/m. The experimental condition maintains equivalently such as compliance tail fin.

Table 5.2 Experiment result (The rigid fin)

Condition	Thrust(mN)
Non Spring 3	367
Non Spring 3.5	378
Non Spring 4	375
Spring 3	472
Spring 3.5	475
Spring 4	488

As Table 5.2 shown, the average thrust of the S case also lager than NS case. The precise explain of the result is similar to the compliance case. From the experimental result, the adjustable Scotch yoke mechanism generates more large thrust than the conventional mechanism regardless of the influence of the compliance.

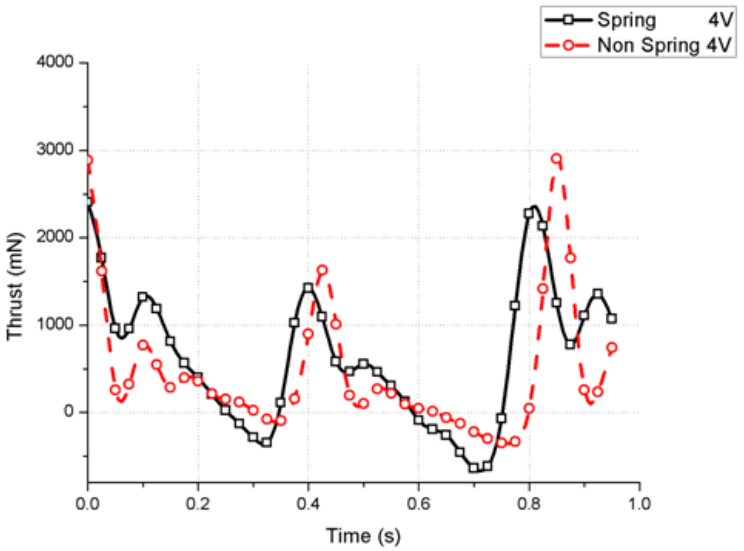

(a)

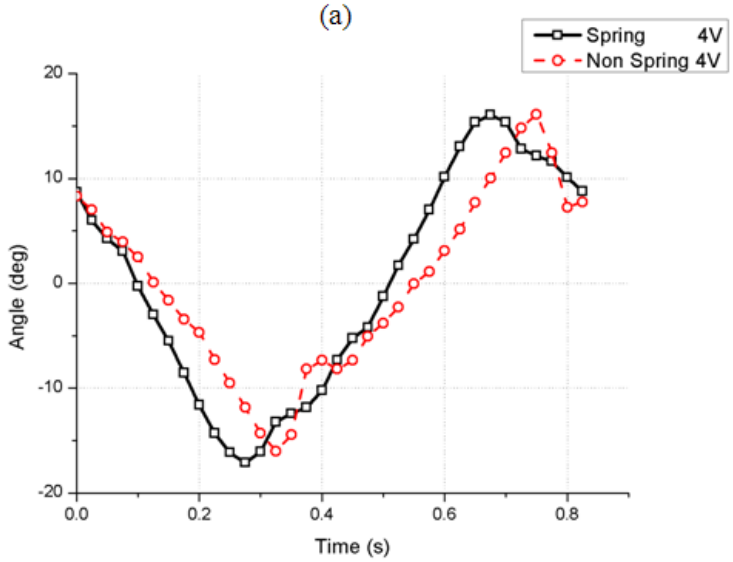

(b)

Figure. 5.2 Graphical synopsis of experimental result (More rigid tail fin) (a) The angle displacement of result (b) The thrust result.

As shown Fig 5.2 (a), in the all case, the maximum thrust is different during the one cycle of the movement of the tail fin. This phenomenon is occurred by asymmetry of the tail fin. To make the more rigid tail fin, we attach the 20 carbon fiber sheets. After that, the carbon fiber sheets are heated by 170 degree and pressed by 15Mpa during the 15 minutes in the heat press machine. This phenomenon is occurred by limitation of the making processing. Thus, the bending angle of the tail fin is different from left and right and the thrust also generated dissymmetrically. In addition, note that the difference between the compliance fin and the rigid fin is shown Fig 5.2 (b). In the compliance fin, the velocity of the NS case became the negative value. Contrastively, in the rigid fin, the displacement of the negative value of NS case is decreased since the amount of the bending is smaller than the compliance fin. Nevertheless, the velocity of the NS case fall down almost zero and the thrust also drop highly regardless of decrease of the negative value in the equal area.

In the rigid fin, the average thrust of the S case is larger than NS case similar with the tendency of the compliance tail fin. As a result, the adjustable Scotch yoke mechanism is more efficient method in the propulsion system since this mechanism generates the higher thrust than conventional mechanism.

Chapter 6. Conclusion and Future Work

Based on these result, we conclude that the adjustable Scotch yoke mechanism can regulate the output torque of the motor. This mechanism stores the motor torque to the two springs when the required torque is relatively small and releases this torque when the required torque increases. In order to regulate the phase of the output torque, we designed the curved shape crank wheel similar with the cam mechanism. In this paper, we analyzed a kinematic model of the Scotch yoke mechanism to propose a method of designing the part of the adjustable Scotch yoke mechanism. In addition, we experiment to measure the thrust of tail fin while the equal input voltage of controller is supplied respectively and compare the conventional mechanism and adjustable Scotch yoke mechanism by considering the compliance of the fin.

Using the adjustable Scotch yoke mechanism, the maximum capable torque of the motor is increased in the desired area because the existing motor torque and released torque from the springs is added to each other. As a result, the motor overcomes the phenomenon which decreases the velocity of tail fin when the large torque is applied to the motor. This means that the adjustable Scotch yoke mechanism generates the larger thrust than even before. The experimental results show that the adjustable Scotch yoke mechanism has better performance than the previous Scotch yoke mechanism during the equal power consumption. Therefore, based on these result, the high speed robotic fish can be made by applying the adjustable Scotch yoke mechanism which

regulated the output torque.

In future research, we optimize the phase of the motor torque by changing the position of the crank wheel because this mechanism only proposes the possibility of the improvement the Scotch yoke mechanism. After that, the robotic fish in which the adjustable Scotch yoke mechanism is applied will be made to be simulated in the real test bed. As a result, the robotic fish using this mechanism can be extending the range of operation in the high velocity flow such as a fast running river and a sea.

Bibliography

[1] D. J. Liang, T. Wang, and L. Wen, “Development of a two-joint robotic fish for real-world exploration,” *J. Field Robot*., **vol. 28**, no. 1, pp. 70–79, 2011.

[2] S. Barret, "Propulsive efficiency of a flexible hull underwater vehicle," Ph.D. Thesis, Dept. of Ocean Institute of Technology, Boston, USA, 1996.

[3] H. Hu, “Biologically inspired design of autonomous robotic fish at Essex,” presented at the IEEE *SMC UK-RI Chapter Conf. Adv. Cybernet*. *Syst*., Sheffield, U.K., 2006.

[4] C. Zhou, K.H. Low, “Better Endurance and Load Capacity: An Improved Design of Manta Ray Robot (RoMan-II)”, *Journal of Bionic Engineering*, **vol. 7**, Supplement, 0, p. S137–S144, 2010.

[5] J. Yu, Z. Su, M. Wang, M. Tan, J. Zhang, “Control of Yaw and Pitch Maneuvers of a Multilink Dolphin Robot”, IEEE *Transactions on Robotics*, **vol. 28**. 2, pp. 318 –329, 2012.

[6] A. Cloitre, V. Subramaniam, N. Patrikalakis P. Valdivia y Alvarado, “Design and control of a field deployable batoid robot”, in 2012 4th IEEE *RAS EMBS International Conference on Biomedical Robotics and Biomechatronics (BioRob*), pp. 707 –712, 2012.

[7] Yong-Jai Park, Useok Jeong, Jeongsu Lee, Seok-Ryung Kwon, Ho-Young Kim, and Kyu-Jin Cho, "Kinematic condition for maximizing the thrust of a robotic fish using a compliant caudal fin,"IEEE *Transactions on Robotics*, **vol. 28**, no. 6, pp. 1216 –1227, 2012.

[8] P.Valdivia,Y. Alvarado, and K.Youcef-Toumi, "Performance of machines with flexible bodies designed for biomimetic locomotion in liquid environments,"in Proc. IEEE *Int. Conf. Robot. Autom*, Apr. pp. 3324–3329, 2005.

[9] P. V. y Alvarado and K. Youcef-Toumi, "Design of machines with compliant bodies for biomimetic locomotion in liquid environments," J. *Dyn.Syst., Meas., Control*, **vol. 128**, no. 1, pp. 3–13, 2006.

[10] C. J. Esposito, J. L. Tangorra, B. E. Flammang, and G. V. Lauder, "A robotic fish caudal fin: Effects of stiffness and motor program on locomotor performance," J. *Exp. Biol*., **vol. 215**, no. 1, pp. 56–67, 2012.

[11] J. Tangorra, C. Phelan, C. Esposito, and G. Lauder, "Use of biorobotic models of highly deformable fins for studying the mechanics and control of fin forces in fishes," *Integr. Comput. Biol*., **vol. 51**, no. 1, pp. 176–189, 2011.

[12] K. H. Low and C. W. Chong, "Parametric study of the swimming performance of a fish robot propelled by a flexible caudal fin," *Bioinsp. Biomimetics*, **vol. 5**, no. 4, p. 046002, 2010.

[13] Yong-Jai Park, Useok Jeong, Jeongsu Lee, Ho-Young Kim and Kyu-Jin Cho, "The effect of compliant joint and caudal fin in thrust generation for robotic fish,", *Biomedical Robotics and Biomechatronics (BioRob), 2010 3rd IEEE RAS and EMBS International Conference on, 26-29 Sept*. pp.528-533, 2010.

[14] J. Yu, Y. F. Li, Y. Hu, L. Wang, "Towards development of link-based robotic dolphin: Experiences and lessons", in IEEE *International Conference on Robotics and Biomimetics, 2008*, pp. 240 –245, 2009.

[15] P. Liu, K. He, X. Ou R. Du, "Mechanical design, kinematic modeling and simulation of a robotic dolphin", in 2011 IEEE *International Conference on Information and Automation (ICIA)*, pp. 738 –743,2011.

[16] R. Fan, J. Yu, L. Wang, G. Xie, Y. Fang, and Y. Hu, "Optimized design and implementation of biomimetic robotic dolphin," in Proc. IEEE *Int.Conf. Robot. Biomimetics*, pp. 484–489, 2005.

[17] W.D. Sauerwein, "Scotch yoke having a curved track, "U.S. Patent 4,272,996, June 1981

[18] J. Yu, Y. Hu, J. Huo, and L. Wang, "Dolphin-like propulsive mechanism based on an adjustable Scotch yoke," *Mechanism and Machine Theory,* **vol. 44**, pp. 603-614, 2009.

[19] Y. Hu, L. Wang, J. Yu, J. Huo, Y. Jia, "Development and control of dolphin-like underwater vehicle", *in American Control Conference,* , pp. 2858 –2863, 2008.

[20] S. Wolf, G. Hirzinger, “A new variable stiffness design: Matching requirements of the next robot generation”, in IEEE *International Conference on Robotics and Automation, 2008. ICRA 2008*, pp. 1741 – 1746, 2008.

국 문 초 록

출력 토크 조절이 가능한 Scotch yoke 메커니즘

일반적으로 로봇물고기를 구동시키기 위하여 사용되는 서보모터는 꼬리지느러미가 왕복운동을 하기 위해 모터의 구동방향을 변경하면서, 모터의 속도가 줄어들게 되어 꼬리지느러미를 높은 주파수로 구동시키는데 어려움이 있다. 따라서 이러한 단점을 해결하기 위하여 Scotch yoke 메커니즘이라는 회전운동을 왕복운동으로 바꿔주는 메커니즘을 사용하여 높은 성능의 DC모터를 이용한 빠른 주파수로 움직일 수 있는 로봇물고기를 제작하게 되었다. 그러나 DC모터는 일정하게 토크를 낼 수 있는 것에 비해 Scotch yoke 메커니즘을 사용하는 경우 모터에 작용하는 토크가 꼬리지느러미의 위상에 따라 다르게 걸리게 된다. 따라서 이번 연구는 상대적으로 모터에 토크가 작게 걸리는 구간에서 스프링에 에너지를 저장하였다가, 토크가 크게 걸리는 구간에서 방출하여 모터의 출력 토크를 조절할 수 있는 Scotch yoke 메커니즘을 제안하였다. Scotch yoke 메커니즘을 사용하여 꼬리지느러미를 구동하는 DC모터에 걸리는 토크를 모델링하여 설계를 위한 변수를 얻었으며, 모터가 낼 수 있는 최대 토크를 제한하여 같은 에너지를 소모하게 하면서 추력을 측정하는 실험을 통하여 기존의

메커니즘과 비교를 하였다. 실험 결과 기존의 메커니즘에서는 모터가 낼 수 있는 토크보다 토크가 크게 걸리는 구간에서 속도가 느려지게 되어 추력이 크게 감소하였으나, 모터의 출력토크를 조절할 수 있는 메커니즘에서는 같은 구간에서 스프링에 저장된 에너지가 더해져 속도가 유지되어 추력이 더 크게 생성되었다. 따라서 향후 이 연구에서 제안된 모터의 토크를 효율적으로 사용할 수 있는 Scotch yoke 메커니즘이 적용한 로봇물고기를 개발할 수 있을 것이다.

주요어: Scotch yoke 메커니즘, 로봇물고기, 출력 토크 조절, 추진 방법,

학 번: 2011-20683